A NON-UNIFORM SUBBAND IMPLEMENTATION OF AN ACTIVE NOISE CONTROL SYSTEM FOR SNORING REDUCTION

Stefano Nobili, Alessandro Nicolini, Ferruccio Bettarelli

Leaff Engineering Srl
Ancona, IT
bettarelli@leaff.it

Valeria Bruschi, Stefania Cecchi

Dept. of Information Engineering
Università Politecnica delle Marche
Ancona, IT
s.cecchi@staff.univpm.it

ABSTRACT

The snoring noise can be extremely annoying and can negatively affect people's social lives. To reduce this problem, active noise control (ANC) systems can be adopted for snoring cancellation. Recently, adaptive subband systems have been developed to improve the convergence rate and reduce the computational complexity of the ANC algorithm. Several structures have been proposed with different approaches. This paper proposes a non-uniform subband adaptive filtering (SAF) structure to improve a feedforward active noise control algorithm. The non-uniform band distribution allows for a higher frequency resolution of the lower frequencies, where the snoring noise is most concentrated. Several experiments have been carried out to evaluate the proposed system in comparison with a reference ANC system which uses a uniform approach.

1. INTRODUCTION

Snoring is a sleep disorder that affects most of the population and produces an annoying noise, which can reach a sound level of 90 dB. Several problems can arise when people's sleep is disturbed by snoring noise. The quality of sleep can decrease, causing loss of productivity, reduction of attention, and unsafe driving [1, 2]. Recent studies have underlined the substantial similarity between snoring and vocal signals [3,4], since both signals present a fundamental frequency followed by high-order harmonics [4]. In particular, the snoring activity can be distinguished into two periods: the inspiration and the expiration. The former produces a signal contained between 100 Hz and 200 Hz, and the latter is concentrated in the frequency range between 200 Hz and 300 Hz. Therefore, the fundamental frequency that must be canceled is located between 100 Hz and 300 Hz.

The snoring attenuation can be achieved by passive or active systems. Passive solutions are based on the use of devices such as earplugs or specific pillows [5]. However, the application of external devices could be very annoying for the user. Moreover, passive techniques do not guarantee a good attenuation of the low frequencies. Differently, active noise control (ANC) methods are more effective with low-frequency noise and are less expensive than passive approaches. ANC systems exploit adaptive filters that can be updated according to the time variations of the acoustic path. The adaptive filters can be designed in several ways. The least mean square (LMS) algorithm and its variants are among the most popular adaptive algorithms. In particular, the normalized least mean square (NLMS), which normalizes the step size with respect to the input signal power, allows to obtain a better convergence than the LMS for non-stationary signals, such as speech [6]. In fact, a faster convergence can be obtained for the same mean squared error (MSE) level once the algorithm has reached convergence. The ANC system introduces a secondary sound source for reproducing an "antinoise" signal. In this way, the primary path is the acoustic path between the noise source and the error microphone, located in the canceling zone, while the secondary path defines the way between the canceling loudspeaker and the error microphone. Typically, such ANC systems are developed using the filtered-x least mean square (FxLMS) algorithm, introduced by Morgan in [7]. The FxLMS structure considers the secondary path impulse response, which is used to filter the input signal, as shown in Fig. 1, improving the performance of the ANC system. Clearly, depending on the input signal that needs to be processed, some variants can be adopted to improve performance such as filtered-x normalized least mean square (FxNLMS).

Focusing on snoring signals, Kuo et al. have proposed in [8] for the first time the use of active snoring cancellation system employing the FxLMS algorithm. Based on this study, other works have recently proposed [2, 9, 10]. Both in [2] and [9], the implementation of FxLMS algorithm in a DSP embedded platforms has been presented proving the effectiveness of ANC with snoring signals and carrying out several real-time experiments. In [10], a multi-channel FxLMS system has been considered using an innovative setup, where the error microphones are placed inside the pillow, instead of on the headboard, enhancing the noise reduction. More recently, an efficient approach based on a delayless subband adaptive filter architecture [11] integrated into a FxLMS algorithm has been presented for snoring cancellation in [12] and a real time implementation of this system has been presented in [13]. However, these approaches consider a uniform band division, inconsistent with the human perception of sound that has a fractional-octave resolution [14].

In this context, this paper proposes for the first time the use of a non-uniform filter bank for active snoring cancellation. The aim is to reach good performance in terms of convergence reducing the number of subbands, and thus the computational cost. The non-uniform filter bank allows for a higher frequency resolution at the low frequencies, where most of the energy of the snoring signal is concentrated. For this reason, this solution guarantees a high convergence rate with a reduced number of subbands, in comparison with the uniform subband approach of [11].

The paper is organized as follows. Section 2 describes the proposed algorithm. Section 3 analyzes the experimental results obtained by using first white noise, and then three different snoring noises. Finally, conclusions are reported in Section 4.

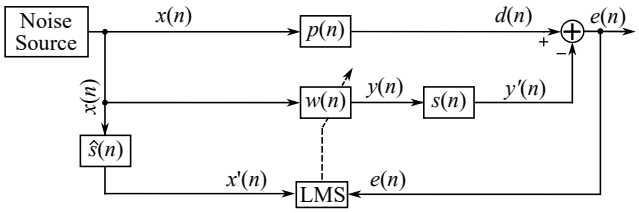

Figure 1: *Scheme of an ANC system based on FxLMS algorithm.*

2. ALGORITHM DESCRIPTION

The general scheme of an ANC system based on FxLMS algorithm is depicted in Fig. 1. The noise signal $x(n)$ reaches the error microphone passing through the primary acoustic path $p(n)$, defining the desired signal $d(n)$. The signal $x(n)$ is filtered by the adaptive filter $w(n)$, obtaining $y(n)$, reproduced by the canceling loudspeaker. Hence, the signal $y(n)$ is propagated through the secondary path $s(n)$ and arrives at the error microphone as $y'(n)$. The error $e(n)$ is defined as

$$e(n) = d(n) - y'(n), \tag{1}$$

and it represents the signal captured by the error microphone. The adaptive filter $w(n)$ is updated by elaborating the residual noise $e(n)$ through the LMS algorithm. Starting from this general approach, the proposed algorithm is shown in Fig. 2. The proposed ANC system implements a SAF structure, derived from the modification of the uniform filter bank used in [12] into a non-uniform filter bank. The creation of the non-uniform filter bank, the subband filter update algorithm, and the procedure for deriving the fullband filter are described in the following.

2.1. Non-Uniform DFT Filter Bank

The non-uniform DFT filter bank is designed as an octave filter bank with $M = 10$ bands. It is obtained from a prototype filter $q(n)$ of length $L_0 = 2048$ and normalized cut-off frequency of π/N_0, where $N_0 = 2^{(M-1)} = 512$. The windowing method using the Hamming window is chosen for the filter design. The first filter of the bank is computed as follows:

$$h_0(n) = q(n)\sqrt{N_0}. \tag{2}$$

The mth filter of the filter bank, with $m = 1, ..., M-1$, is calculated as follows:

$$h_m(n) = q(kn)\sqrt{kN_0}e^{j\left(\frac{2\pi k}{N_0}\right)n}, \tag{3}$$

where $k = 2^{(m-1)}$, $n = 0, ..., L_m - 1$, and $L_m = L_0/k$ defines the length of the mth filter. In this way, the longest filters, with 2048 coefficients, describe the first and second bands, while the length of each following filter is progressively reduced by two, arriving at the shortest filter of the tenth band composed of 8 taps.

2.2. Subband Adaptive Filtering

The input signal $x(n)$ is processed through the estimated secondary path $\hat{s}(n)$, yielding the reference signal $x'(n)$. Typically, the estimated $\hat{s}(n)$ may deviate from the actual secondary path $s(n)$, and such estimation is generally performed offline. However, for this study, we assume an ideal case where $\hat{s}(n) = s(n)$

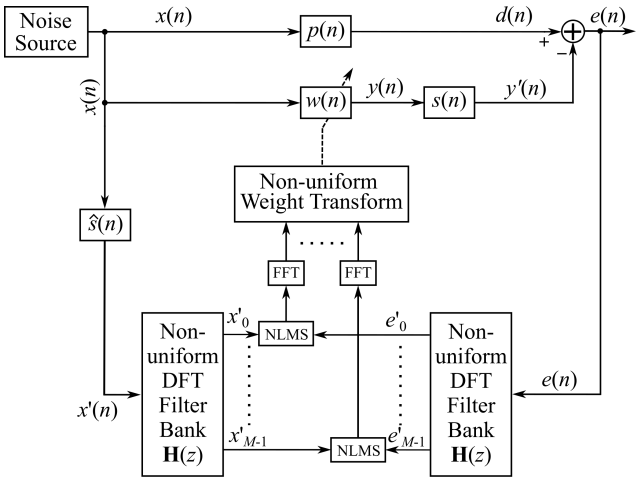

Figure 2: *Structure of the proposed ANC approach with delayless non-uniform subbands algorithm.*

[15]. The non-uniform filter bank is applied to $x'(n)$ and to the error signal $e(n)$, obtaining the respective subband signals $x'_m(n)$ and $e'_m(n)$, with $m = 0, 1, ..., M-1$. The weights of the m-th subband $\mathbf{w}_m^{\text{SAF}}(n)$ are calculated using the normalized LMS (NLMS) algorithm as

$$\mathbf{w}_m^{\text{SAF}}(n+1) = \mathbf{w}_m^{\text{SAF}}(n) + \mu_m \mathbf{x}'^{*}_m(n) e'_m(n), \tag{4}$$

where $*$ denotes the complex conjugation. μ_m is the step size normalized by the power of the mth band signal as follows:

$$\mu_m = \frac{\mu}{\alpha + ||\mathbf{x}'_m(n)||^2}, \tag{5}$$

where α is a small number to avoid division by zero and μ is the step size. The final fullband filter is obtained through the weight transformation described in the following section.

2.3. Weight Transformation

The weight transformation is applied to the adaptive subfilters to obtain an equivalent real-valued fullband filter of length L. The transformation is achieved by implementing the following steps:

- the subband weights are transformed by (L/D_m)-point FFT, where $D_m = N_0/(2k)$ is the mth decimation factor with $k = 2^{(m-1)}$ for $m = 1, ..., M-1$, and $D_0 = N_0/2$;

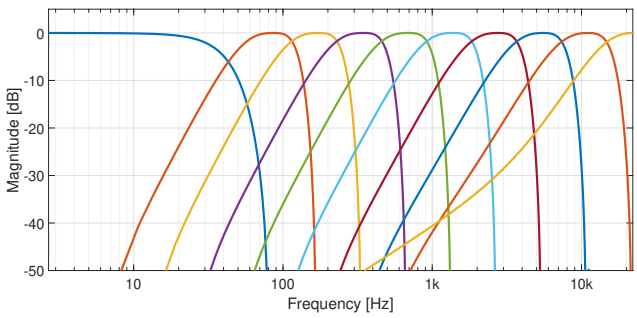

Figure 3: *Non-uniform filter bank used in the proposed system. The x-axis is reported on a logarithmic scale.*

- the complex samples of FFT are stacked in the right position of the array of the fullband complex filter;
- to complete the array, the central point is set to zero and the samples stacked in the first half are complex conjugate and reverse in order to fill the position of the second half of the array;
- the fullband filter $w(n)$ is calculated by a $2L$-point inverse FFT (IFFT) of the array and the final fullband filter is obtained by the first L coefficients of the result.

3. EXPERIMENTAL RESULTS

The proposed system has been validated through several simulations, carried out on MATLAB. For the experiments, the primary path $p(n)$ and the secondary path $s(n)$ have been measured in a semianechoic environment following the setup described in [9] and shown in Figure 4. In particular, the reference microphone is placed close to the noise sound source to capture the input signal $x(n)$. Additionally, a distance of 2 m between the noise source and the error microphone (primary path) and 20 cm between the canceling loudspeaker and the error microphone (secondary path) have been considered. The impulse response of the primary path is 1024 samples, while the secondary path is 512 samples. A sampling frequency of $f_s = 44.1$ kHz has been used.

In the experiments, the proposed approach with the non-uniform filter bank is compared with the case of the uniform filter bank of [11]. The non-uniform filter bank is composed of $M = 10$ bands, shown in Figure 3. The subband filters have different lengths for each band, i.e., [2048, 2048, 1024, 512, 256, 128, 64, 32, 16, 8], from the first to the tenth band, respectively. The uniform filter bank is applied using 64 subbands of equal frequency width and subband filters of length 384 samples, to guarantee a computational cost comparable to the proposed approach. For both approaches, the length of the fullband adaptive filter $w(n)$ is 1024, and the factor α of Equation (5) is set to $\alpha = 10^{-6}$.

First, the algorithm has been tested using white noise as input to analyze the performance with broadband noise and to control all the frequencies between adjacent bands with different cutoff frequencies. After that, three different snoring signals are applied to the proposed system.

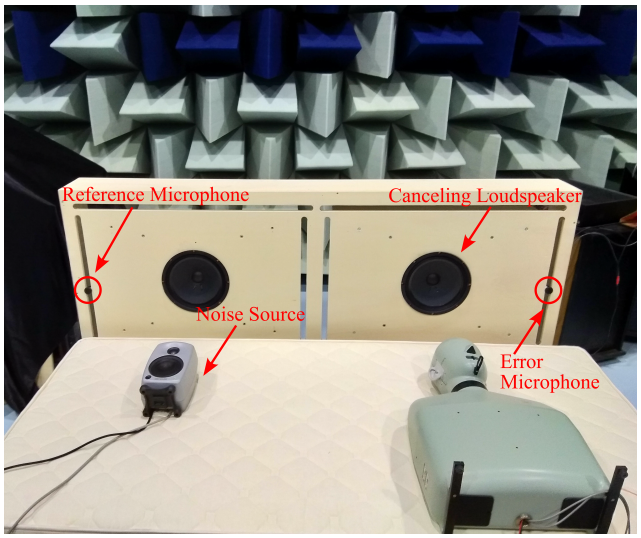

Figure 4: *Photo of the setup used for the experiments.*

3.1. Validation with White Noise

The validation test has been carried out with many simulations to find the optimal values of step size for the adaptive algorithm. In particular, a step size of $\mu = 0.1$ has been chosen for both the uniform and the non-uniform filter bank. In Figure 5, the responses of the primary path estimated with the uniform and the non-uniform ANC algorithm are compared to the measured one in both the time and the frequency domain. The non-uniform filter-bank produces a better estimation, especially at low frequencies, where subband filters have a narrower width. Figure 6 reports the mean squared errors compared to the input noise signal. The final residual error is comparable between the two methods, however, the non-uniform case guarantees a higher convergence speed.

3.2. Results with Snoring Noise

After the validation with white noise presented in Section 3.1, the proposed algorithm has been tested considering snoring noise signals as input. The snoring signals have been analyzed to evaluate the frequency power distributions, shown in Figures 7(a), 7(b), and 7(c). As said above, the major part of the energy of this type of signal is concentrated in the medium and lower frequencies, and the filter bank has been designed considering this power distribution.

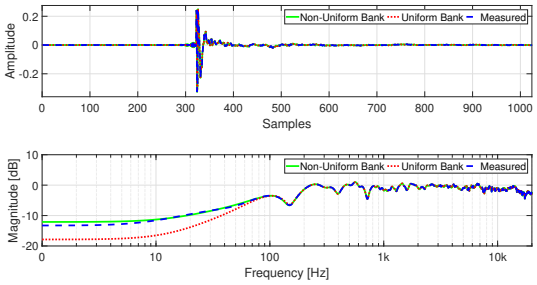

Figure 5: *Impulse response comparison between the proposed approach and the reference algorithm of [11], taking into consideration the original measured impulse response.*

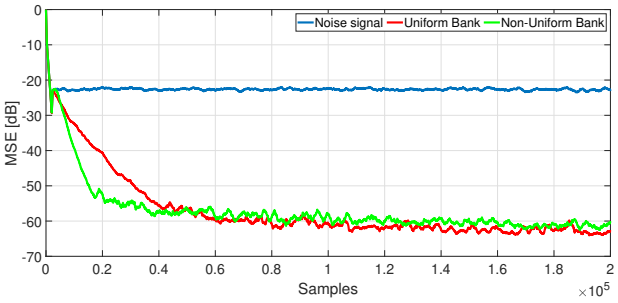

Figure 6: *MSE comparison considering the original noise signal and the noise cancellation obtained with the proposed approach and with the reference algorithm of [11]*

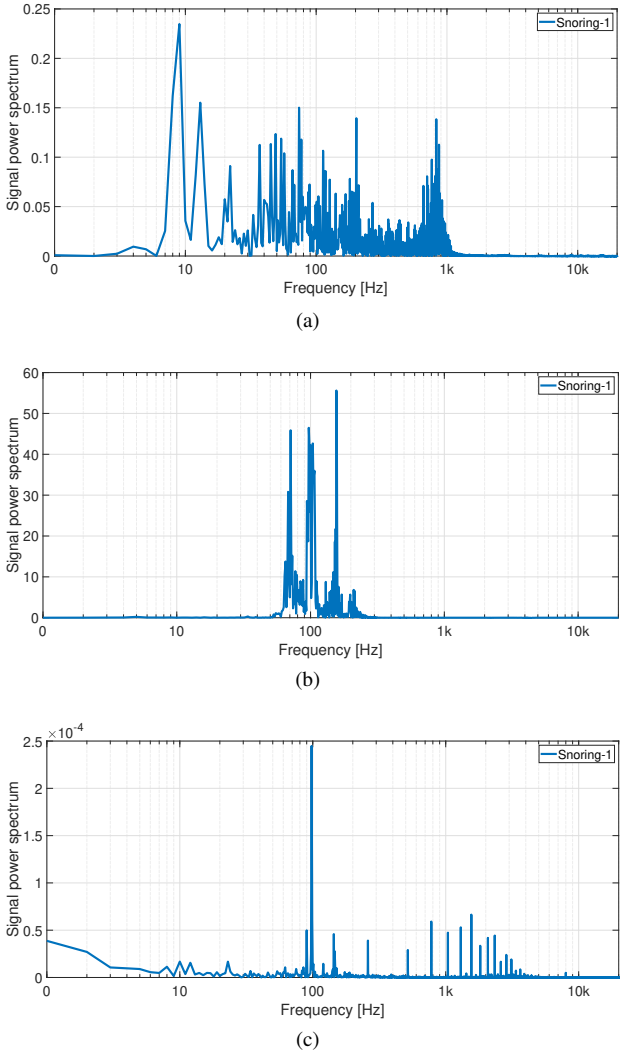

Figure 7: *Amplitude spectrum of (a) the first, (b) the second, and (c) the third snoring signal, used for the experiments.*

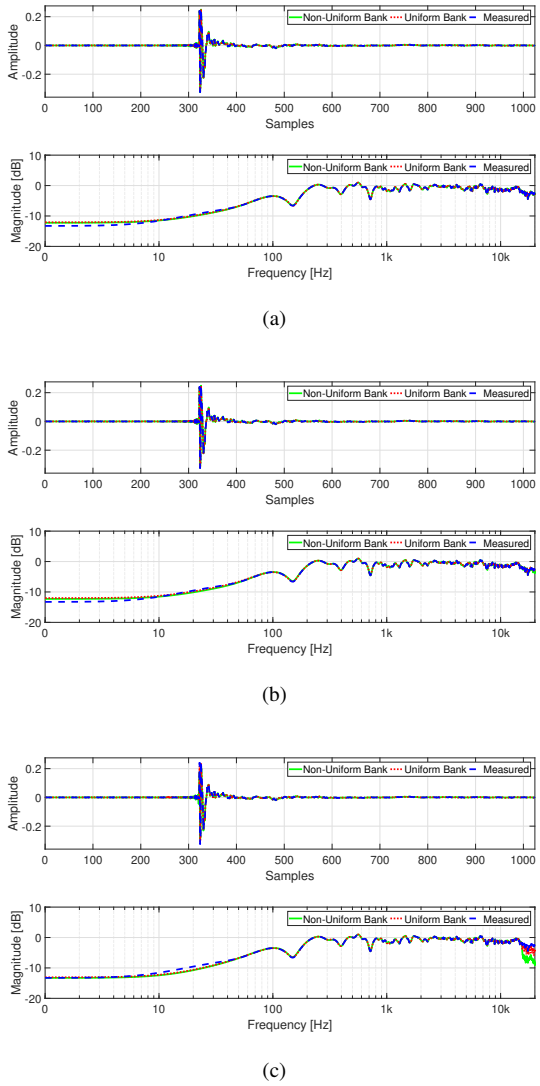

Figure 8: *Impulse response comparison between the proposed approach filter, the reference approach of [11], and the measured impulse response considering as input (a) the first, (b) the second and (c) the third snoring signals.*

In particular, the first signal (Figure 7(a)) contains most of the energy in the band between 10 Hz and 1 kHz. The second snore (Figure 7(b)) has a narrower band between 60 Hz and 200 Hz. Finally, the third signal (Figure 7(c)) has a huge contribution at 100 Hz and minor peaks up to 3 kHz.

Also in this case, several simulations have been achieved to find the optimal values of step size. Defining as μ_u the step size of the uniform approach and as μ the step size of the proposed non-uniform method, the following values have been used for the three signals:

- for Snoring-1, μ_u=0.05, and $\mu = 0.05$;
- for Snoring-2, μ_u=0.1, and $\mu = 0.05$;
- for Snoring-3, μ_u=0.03, and $\mu = 0.05$.

As it can be seen, for the non-uniform case, there was no need to change the step size since the best results are always obtained with $\mu = 0.05$.

Figure 8 shows the estimated primary paths compared to the measured one both in time and in the frequency domain for all three cases. Figure 9 shows the MSE values of the uniform and non-uniform approach in comparison with the mean squared noise input signal. Finally Figure 10 shows the residual error signals compared to the input snoring noise.

In detail, with the first snore, the primary path is perfectly reconstructed with both uniform and non-uniform filter banks. However, the MSE plot of Figure 9(a) reveals a faster convergence of the non-uniform approach. The two algorithms reach the same MSE values around 250k samples. This is also confirmed by the error trends shown in Figure 10(a).

Similar observations can be derived from the results obtained with the second snoring. The primary path is correctly esti-

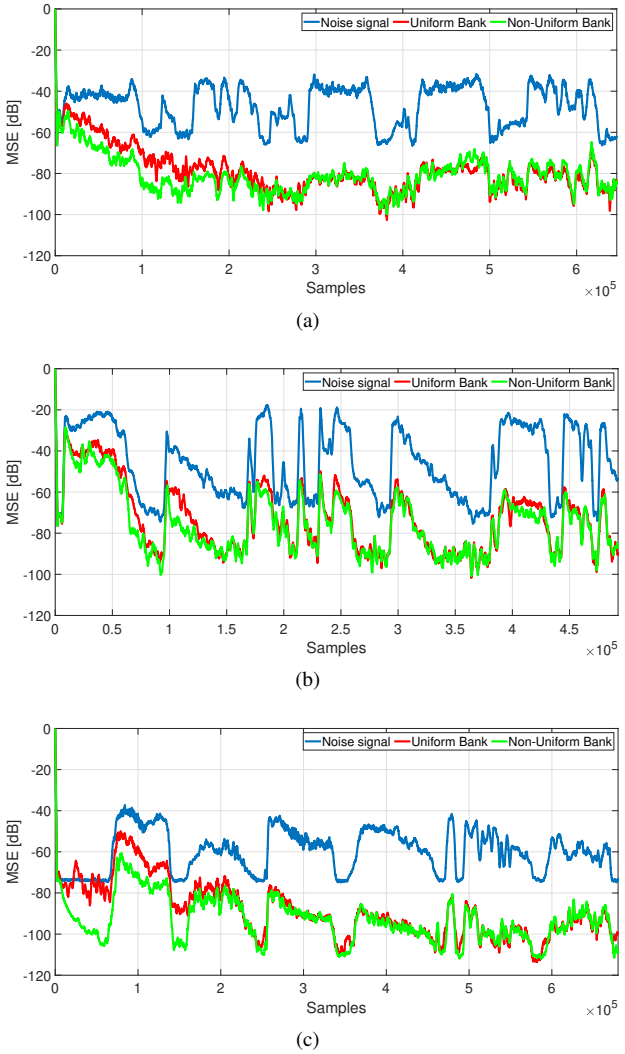

Figure 9: *MSE comparison considering the original noise signal and the effect of noise cancellation with the proposed approach and with the approach of [11] for (a) the first, (b) the second and (c) the third snoring signals.*

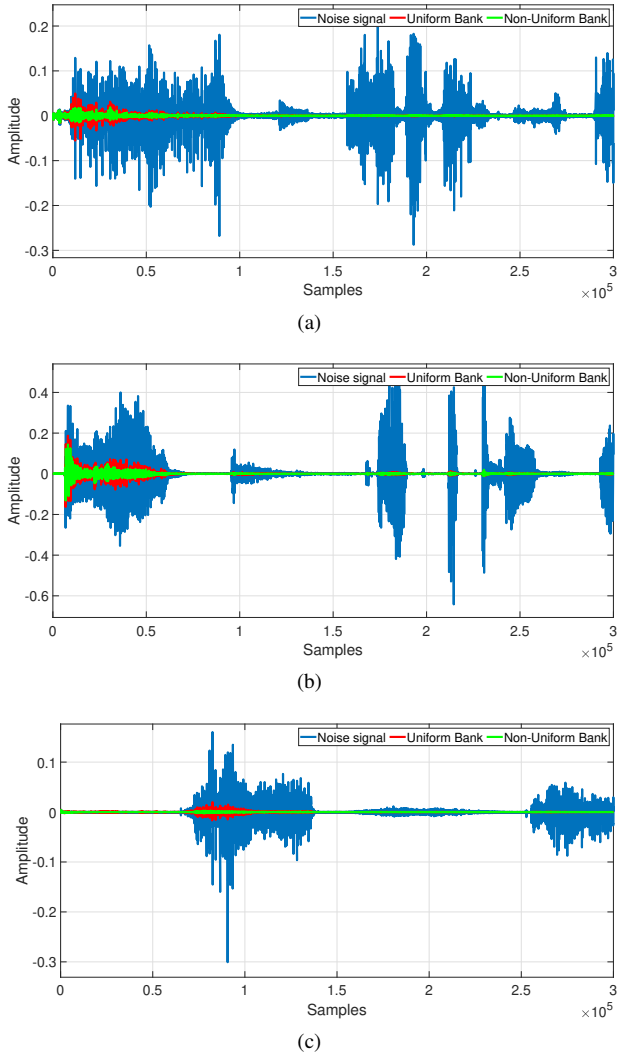

Figure 10: *Comparison considering the original noise signal and the effect of noise cancellation with the proposed approach and with the approach of [11] for (a) the first, (b) the second and (c) the third snoring signals.*

mated, as shown in Figure 8(b) because the adaptation algorithm is stopped when both approaches reach the minimum error. Then again, the MSE value of Figure 9(b) shows a lower error for the non-uniform technique, especially in the parts where the signal is greater, i.e., when the snoring occurs. Figure 10(b) shows the comparison between the two residual errors proving the better cancellation of the proposed approach.

Finally, the estimated paths with the third snoring signal are shown in Figure 8(c). The impulse response is correctly reconstructed up to 15 kHz with both algorithms. Looking at the MSE value of Figure 9(c), it is evident that the non-uniform bank guarantees a greater convergence rate. This result is also clearly visible in the residual signal of Figure 10(c).

4. CONCLUSIONS

In this paper, an active noise control system based on a non-uniform subband implementation is proposed. The non-uniform octave-band DFT filter bank is used in the FxNLMS structure to filter the reference and the error signals. The subband adaptive filters are updated using the NLMS algorithm, and the final full-band adaptive filter is reconstructed through a weight transformation procedure. The proposed system has been compared with an existing state-of-the-art approach that uses a uniform filter bank. First, a validation of the proposed approach has been carried out considering white noise as input. Then, three snoring signal are used to evaluate the performance in terms of the reconstructed impulse response, mean squared error, and residual error. In all the cases, the non-uniform approach allows for faster convergence, ensuring a good noise reduction before the ANC with the uniform

filter bank. Future works will be focused on real-time implementation and testing of the proposed algorithm exploiting a DSP platform.

5. REFERENCES

[1] S. R. Chakravarthy and S. M. Kuo, "Application of active noise control for reducing snore," in *Acoustics, Speech, and Signal Processing, 1988. ICASSP-88., 1988 International Conference on*, 06 2006, vol. 5, pp. V – V.

[2] C. Y. Chang, S. T. Pan, and K. C. Liao, "Active noise control and its application to snore noise cancellation," *Asian Journal of Control*, vol. 15, 11 2013.

[3] R. Beck, M. Odeh, A. Oliven, and N. Gavriely, "The acoustic properties of snores," *European Respiratory Journal*, vol. 8, no. 12, pp. 2120–2128, 1995.

[4] D. Pevernagie, R. M. Aarts, and M. De Meyer, "The acoustics of snoring," *Sleep Medicine Reviews*, vol. 14, no. 2, pp. 131–144, 2010.

[5] R. Wei, H. S. Kim, X. Li, J. J. Im, and H. J. Kim, "A development of mechanism for reducing snoring," in *2010 International Conference on Electronics and Information Engineering*, 2010, vol. 2, pp. V2–242–V2–245.

[6] K. A. Lee, W. S. Gan, and S. M. Kuo, *Subband adaptive filtering: Theory and implementation*, John Wiley & Sons, 2009.

[7] D. Morgan, "An analysis of multiple correlation cancellation loops with a filter in the auxiliary path," *IEEE Transactions on Acoustics, Speech, and Signal Processing*, vol. 28, no. 4, pp. 454–467, 1980.

[8] S. M. Kuo and R. Gireddy, "Real-time experiment of snore active noise control," in *2007 IEEE International Conference on Control Applications*, 2007, pp. 1342–1346.

[9] S. Cecchi, A. Terenzi, P. Peretti, and F. Bettarelli, "Real time implementation of an active noise control for snoring reduction," in *Proc. 144th Audio Engineering Society Convention*. Audio Engineering Society, 2018.

[10] L. Liu, K. R. Pottim, and S. M. Kuo, "Ear field adaptive noise control for snoring: an real-time experimental approach," *IEEE/CAA Journal of Automatica Sinica*, vol. 6, no. 1, pp. 158–166, 2019.

[11] R. M. Morgan and J. C. Thi, "A Delayless Subband Adaptive Filter Architecture," *IEEE Trans. Signal Process*, vol. 43, no. 8, pp. 1819–1830, Aug. 1995.

[12] S. Nobili, V. Bruschi, F. Bettarelli, and S. Cecchi, "An efficient active noise control system with online secondary path estimation for snoring reduction," in *2021 29th European Signal Processing Conference (EUSIPCO)*. IEEE, 2021, p. 7.

[13] S. Nobili, V. Bruschi, F. Bettarelli, and S. Cecchi, "A real time subband implementation of an active noise control system for snoring reduction," in *2021 12th International Symposium on Image and Signal Processing and Analysis (ISPA)*. IEEE, 2021, pp. 109–114.

[14] P. D. Hatziantoniou and J. N. Mourjopoulos, "Generalized fractional-octave smoothing of audio and acoustic responses," *Journal of the Audio Engineering Society*, vol. 48, no. 4, pp. 259–280, 2000.

[15] M. K. Kuo and R. M. Morgan, "Active Noise Control: a Tutorial Review," *Proc. IEEE*, vol. 87, no. 6, pp. 943–973, Jun. 1999.